Synthesis of single-qutrit circuits from Clifford+*R* gates

Erik J. Gustafson,[1,2,3,4,*] Henry Lamm,[1,2,†] Diyi Liu,[5,‡] Edison M. Murairi,[1,2,6,§] and Shuchen Zhu[7,8,‖]

[1]*Superconducting and Quantum Materials System Center (SQMS), Batavia, Illinois 60510, USA*

[2]*Fermi National Accelerator Laboratory, Batavia, Illinois 60510, USA*

[3]*Quantum Artificial Intelligence Laboratory (QuAIL), NASA Ames Research Center, Moffett Field, California 94035, USA*

[4]*USRA Research Institute for Advanced Computer Science (RIACS), Mountain View, California 94043, USA*

[5]*School of Mathematics, University of Minnesota-Twin Cities, Minneapolis, Minnesota 55414, USA*

[6]*Department of Physics, The George Washington University, Washington, DC 20052, USA*

[7]*Department of Mathematics, Duke University, Durham, North Carolina 27708, USA*

[8]*Duke Quantum Center, Duke University, Durham, North Carolina 27701, USA*

(Received 4 April 2025; revised 1 October 2025; accepted 13 November 2025; published 8 December 2025)

We present two deterministic compilation algorithms for single-qutrit unitaries with $O(\log 1/\varepsilon)$ gate depth. Each algorithm selects a nearby approximation to the target unitary and then exactly synthesizes the approximation over the Clifford + **R** basis. The first algorithm exhaustively searches over the group; while the second algorithm searches only for Householder reflections. The exhaustive search algorithm yields an average **R** count of $2.193(11) + 8.621(7)\log_{10}(1/\varepsilon)$, albeit with a time complexity of $O(\varepsilon^{-4.4})$. The Householder search algorithm results in a larger average **R** count of $3.20(13) + 10.77(3)\log_{10}(1/\varepsilon)$ at a reduced time complexity of $O(\varepsilon^{-0.42})$, greatly extending the reach in ε. These costs correspond asymptotically to 35% and 69% more non-Clifford gates compared with synthesizing the same unitary with two qubits. Such initial results are encouraging for using the **R** gate as the nontransversal gate for qutrit-based computation.

DOI: 10.1103/98q1-3yv8

I. INTRODUCTION

Various fields anticipate that quantum computing will tackle problems that are intractable for classical computers, but the large-scale architecture is still an active area of study. While most devices are qubit-based, many have access to higher levels and thus could be run as qudit-based platforms, including trapped ions [1–3], transmons [4–12], Rydberg arrays [13,14], photonic circuits [15], cold atoms [16,17], and superconducting radio frequency (SRF) cavities [18]. While experimentally more challenging, there are advantages to developing qudit-based systems from an algorithmic perspective due to their enhanced effective connectivity, as native single-qudit SU(d) rotations replace nonlocal multiqubit circuits [19–22]. In practice, this allows for lower gate fidelities for the same algorithmic fidelity [11,23–32]. Such potential has led to application-specific research in qudits across fields such as material science [33–37], numerical optimization [38–41], condensed matter [42–46], and particle physics [47–56].

Regardless of the qudit dimensionality, reaching the goal of quantum utility requires fault-tolerant gate synthesis. That is, one identifies a finite set of generators that can efficiently approximate unitary operations to any required precision and support quantum error correction for the logical gates in the set. Fundamentally, though, the Eastin-Knill theorem [57] prevents a universal gate set that is also transversal, i.e., not all logical gates can be implemented in parallel across the physical qudits. This constrains the gate sets $\mathcal{G}$ for large-scale computation. Furthermore, the nontransversal gate counts $N_{\mathcal{G}}$ dominate the computation costs [58], but recent evidence suggests they may not be as expensive as thought [59,60]. Here, we take the first steps beyond qubits by considering the fault-tolerant gate synthesis of $d = 3$ qudits, called *qutrits*.

The prevalence of the qubits extends to fault-tolerant gate synthesis. There, the Clifford group extended by $\mathbf{T} = \mathrm{Diag}(1, e^{i\pi/4})$—denoted $(\mathbf{C} + \mathbf{T})_2$—is the leading choice. However, novel sets with non-Clifford transversal operations [61–63] or those based on groups larger than the Clifford group also exist [64–66]. Once this finite gate set is selected, one must map all other circuit primitives to a gate set *word*. While $(\mathbf{C} + \mathbf{T})_2$ does not result in the shortest word lengths compared with larger groups [65–68], it has well-established error correction schemes and experimental demonstrations, in contrast with other gate sets and codes. In the case of qutrits, three options have dominated the literature, which extend the qutrit-Cliffords $\mathbf{C}_3$, although others exist [69,70]. The first uses the generalized $\mathbf{T}_3 = \mathrm{Diag}(1, \omega, \omega^2)$ [71–75] where $\omega = e^{2\pi i/3}$ is the third root of unity. The other two common extensions are $\mathbf{D}(a, b, c) = \mathrm{Diag}(\pm\xi^a, \pm\xi^b, \pm\xi^c)$ [76–78], where $\xi = e^{2\pi i/9}$, and the metaplectic $\mathbf{R} = \mathrm{Diag}(1, 1, -1)$ [79,80] gates. While the metaplectic set $(\mathbf{C} + \mathbf{R})_3$ is strictly a subset of $(\mathbf{C} + \mathbf{T})_3$ [80], it may prove more practical in hardware and

*Contact author: egustafson@usra.edu
†Contact author: hlamm@fnal.gov
‡Contact author: liu00994@umn.edu
§Contact author: emurairi@fnal.gov
‖Contact author: shuchen.zhu@duke.edu

thus warrants study. Thus, in this work, we study the synthesis of SU(3) unitaries using $(\mathbf{C}+\mathbf{R})_3$.

The Solovay-Kitaev theorem states that the number of gates necessary for an approximation of a single gate with error ε scales as $O(\log^{\gamma}(\frac{1}{\varepsilon}))$ for some γ that depends on the set and algorithm employed. The only previously known deterministic algorithm known for qutrits is the Solovay–Kitaev algorithm with $\gamma \approx 1.44+\delta$ for some small positive δ [81,82]. Our work improves this situation by producing an algorithm for approximation plus an exact synthesis framework for qutrits by generalizing the modern qubit synthesis approaches based on number theory [79], which guarantees $\gamma = 1$ when constructed over algebraic integers. Beyond γ, we determine the actual prefactor of $\log(1/\varepsilon)$ for $(\mathbf{C}+\mathbf{R})_3$, enabling fault-tolerant resource estimates.

This work is organized as follows: We briefly review qutrit-based computation and ring-based gate synthesis in Sec. II. This leads into Secs. III and IV, where two algorithms are constructed for approximating diagonal single-qutrit gates: the exhaustive search and the Householder search. This is followed by a method for determining the $(\mathbf{C}+\mathbf{R})_3$ word for the approximation in Sec. V. Numerical studies are found in Sec. VI and comparisons between qubit and qutrit compilation are found in Sec. VII. We then conclude in Sec. VIII.

II. THEORETICAL BACKGROUND

Qutrit systems have a basis of three-level states $|0\rangle$, $|1\rangle$, and $|2\rangle$; their Hilbert spaces scale as 3^N which is a polynomial increase compared with the qubits' 2^N. A universal—though not fault-tolerant—gate set for qutrits can be built from single-qutrit rotations and an entangling gate. One such set is the 18 two-level Givens rotations,

$$R^{\alpha}_{(b,c)}(\theta) = e^{-i\theta/2\sigma^{\alpha}_{(b,c)}}, \tag{1}$$

where $\sigma^{\alpha}_{(b,c)}$ is the Pauli matrix $\sigma^{\alpha} = \{X, Y, Z\}$ acting on the $|b\rangle - |c\rangle$ subspace, combined with the CSUM gate:

$$\text{CSUM}|i\rangle|j\rangle = |i\rangle|i \oplus_3 j\rangle. \tag{2}$$

While CSUM is part of qutrit Clifford group, $R^{\alpha}_{(b,c)}(\theta)$ are not. Therefore, if one wants to implement the $R^{\alpha}_{(b,c)}(\theta)$ rotations using a fault-tolerant gate set, one has to approximately synthesize these rotations using a finite set of gates such as $(\mathbf{C}+\mathbf{R})_3$. This approximation is possible due to, i.e., the Solovay-Kitaev theorem [81]—any d-dimensional qudit gate $U \in \text{SU}(d)$ can be approximated by a gate $V \in \mathcal{G}$, with $||U-V|| \leqslant \varepsilon$ and $N_{\mathcal{G}}$ scaling as $O(\log^{a}_{d}(1/\varepsilon))$.

Optimal algorithms correspond to the case where the exponent overhead $a = 1$ [83,84]. Furthermore, by considering the geometric structure of hyperspheres covering SU(d), one can show that there always exists a unitary $U \in \text{SU}(d)$ whose ε-approximation V requires at least [74,85]

$$N_{\mathcal{G}} \gtrsim \frac{\ln(A) + (d^2-1)\ln\left(\frac{1}{\varepsilon}\right)}{\ln(d(d-1))}, \tag{3}$$

where

$$A = \frac{\sqrt{2^{d-1}d}[d(d-1)-1]\,\Gamma\left(\frac{d^2-1}{2}\right)}{d^4\pi^{3/2(d-1)}G(d+1)}, \tag{4}$$

and $G(n) = \prod_{k=1}^{d-1} k!$ is the Barnes G function. For the case of qubits ($d = 2$), Eq. (3) predicts

$$\begin{aligned} N_{\mathcal{G}} &= 3\log_2(1/\varepsilon) - 5.65 \\ &= 9.97\log_{10}(1/\varepsilon) - 5.65. \end{aligned} \tag{5}$$

For qutrits ($d = 3$), we find

$$\begin{aligned} N_{\mathcal{G}} &= 4.9\log_3(1/\varepsilon) - 2.16 \\ &= 10.27\log_{10}(1/\varepsilon) - 2.16. \end{aligned} \tag{6}$$

The described properties are independent of a specific $\mathcal{G}$, meaning that specific instances may exhibit different performance. We focus here on $\mathcal{G} = (\mathbf{C}+\mathbf{R})_3$ which is generated by the qutrit Hadamard H, phase gate S, and $\mathbf{R}$, following the notation of Ref. [76]:

$$\begin{aligned} H &= \frac{1}{i\sqrt{3}}\begin{pmatrix} 1 & 1 & 1 \\ 1 & \omega & \omega^2 \\ 1 & \omega^2 & \omega \end{pmatrix}, \\ S = \text{Diag}(1,\omega,1), &\quad \mathbf{R} = \text{Diag}(1,1,-1). \end{aligned} \tag{7}$$

Other gates in $\mathbf{C}_3$ that will prove useful include:

$$X = \begin{pmatrix} 0 & 0 & 1 \\ 1 & 0 & 0 \\ 0 & 1 & 0 \end{pmatrix}, \quad D(a,b,c) = \text{Diag}(\omega^a, \omega^b, \omega^c), \tag{8}$$

where $a, b, c \in \{0, 1, 2\}$. The decomposition of $D(a, b, c)$ into H, S can be aided by the relations:

$$\begin{aligned} H^{\dagger} = H^3, &\quad X_{(0,1)} = HS^2H^2SH^{\dagger}, \\ X_{(1,2)} = H^2, &\quad \text{and } X = H^{\dagger}SH^2S^2H^{\dagger}, \end{aligned} \tag{9}$$

where $X_{(i,j)}$ acts as a transposition gate in the (i, j) subspace of the qutrit Hilbert space. As an example,

$$D(1,2,1) = X_{(0,1)}SXSX_{(1,2)}S^2. \tag{10}$$

Determining efficient synthesis is an ongoing area of research, even for qubits. The best algorithms rely upon insight from number theory. One can show that any $V \in \mathcal{G}$ consists of matrix entries in a ring $\mathcal{R}$. This was proven and then used to perform exact single-qubit synthesis in $(\mathbf{C}+\mathbf{T})_2$ [86]. The extension to approximate synthesis requires determining a V that is within distance ε of the desired gate.

Identifying these approximations requires solving a Diophantine equation. In general, this is NP-complete [87] and thus finding the shortest word is often difficult. Luckily, this need not prevent subclasses of gates from being approximated efficiently. In particular, a probabilistic number-theoretic method to approximate diagonal single-qubit gates was first introduced in Ref. [88]. Since any single-qubit gate can be exactly represented by three diagonal gates and $\mathbf{C}_2$, it was demonstrated that $U \in \text{SU}(2)$ could be approximated with $N_{\mathcal{G}} = 3\log_p(1/\varepsilon^3)$ with a gate set associated with a prime p. For $(\mathbf{C}+\mathbf{T})_2$ one finds $p = 2$ while other "golden gate sets" can be used to reduce this bound up to $\frac{7}{3}\log_{59}(1/\varepsilon^3)$ [65]. Further improvements have been made for $(\mathbf{C}+\mathbf{T})_2$, with the state-of-the-art being the repeat-until-success method of Ref. [89]. Ultimately, finding ways to decompose and approximate arbitrary gates more efficiently than by diagonal matrices remains an open problem.

Similarly, $(\mathbf{C}+\mathbf{R})_3$ can be related to a localized ring.[1] Starting from the ring of Eisenstein integers, $\mathcal{R}_3 = \{a_0 + a_1\omega \mid a_i \in \mathbb{Z},\ \omega = e^{\frac{2\pi i}{3}}\}$, one localizes it to obtain the ring $\mathcal{R}_{3,\chi} = \{\frac{a}{\chi^f} \mid a \in \mathcal{R}_3,\ f \in \mathbb{N}_0\}$ where $\chi = 1 + 2\omega = \sqrt{-3}$. Inspecting the generators [Eq. (7)], one sees that all their entries are in $\mathcal{R}_{3,\chi}$. Therefore, the set generated by the $(\mathbf{C}+\mathbf{R})_3$ is the unitary group over the $\mathcal{R}_{3,\chi}$ ring, denoted by $U(3, \mathcal{R}_{3,\chi})$ [76,90]. Thus, any matrix $V \in (\mathbf{C}+\mathbf{R})_3$ has the form

$$V = \frac{1}{\chi^f}\begin{pmatrix} x_1 & y_1 & z_1 \\ x_2 & y_2 & z_2 \\ x_3 & y_3 & z_3 \end{pmatrix}, \tag{11}$$

where $x_i, y_i, z_i \in \mathcal{R}_3$, and $f \in \mathbb{N}_0$. An important consequence of this observation is that synthesis over this gate set can be performed with optimal scaling of the number of gates, $O(\log_3(1/\varepsilon))$. The remaining challenge lies in developing a constructive algorithm that reaches this complexity while minimizing constant factors. Such an algorithm can be decomposed into two steps. First, find a sufficient approximation $V \in U(3, \mathcal{R}_{3,\chi})$. Then, determine the $(\mathbf{C}+\mathbf{R})_3$ word that exactly synthesizes V.

Any single-qutrit unitary is a product of a global phase and an SU(3) matrix. Noting that a global phase may be synthesized by a modification of our algorithm, we focus only on SU(3) matrices which can be synthesized using $\mathbf{C}_3$ rotations from

$$R^Z_{(0,1)}(\theta) = \mathrm{Diag}(e^{-i\theta/2}, e^{i\theta/2}, 1). \tag{12}$$

Thus, the goal is to find $V \in U(3, \mathcal{R}_{3,\chi})$ such that

$$\left|\left|R^Z_{(0,1)}(\theta) - V\right|\right| \leqslant \varepsilon, \tag{13}$$

given a choice of θ and an error $\varepsilon > 0$. We use the Frobenius norm[2] throughout this work. Furthermore, anticipating the high cost of implementing non-Clifford gates, we use the number of $\mathbf{R}$ gates, $N_{\mathbf{R}}$, as the quantum complexity of the synthesis problem.

To solve Eq. (13), we present two algorithms. The first algorithm conducts an exhaustive search over $(\mathbf{C}+\mathbf{R})_3$ group, yielding good results but incurring significant classical runtime. The second algorithm restricts its search to Householder reflection gates, improving classical complexity while requiring an increased $N_{\mathbf{R}}$. The following sections provide detailed explanations of both algorithms.

Before describing both algorithms, it is helpful to consider the geometry of the Eisenstein integers within the real plane $\mathbb{R}^2$. Any complex number z (e.g., $e^{i\theta/2}$) can be represented as a vector in $\mathbb{R}^2$ via the mapping

$$z \mapsto \begin{pmatrix} \mathrm{Re}\,(z) \\ \mathrm{Im}\,(z) \end{pmatrix}. \tag{14}$$

In particular, any Eisenstein integer, $x_1 + x_2\omega \in \mathcal{R}_3$, maps to the real vector

$$\mathbf{y} = \begin{pmatrix} x_1 - \frac{x_2}{2} \\ \frac{x_2\sqrt{3}}{2} \end{pmatrix} \in \mathbb{R}^2. \tag{15}$$

As a result, the Eisenstein integers form an integer lattice $\mathcal{L}_1 \subset \mathbb{R}^2$ generated by

$$B_1 = \begin{pmatrix} 1 & -\frac{1}{2} \\ 0 & \frac{\sqrt{3}}{2} \end{pmatrix}, \tag{16}$$

i.e.,

$$\mathcal{L}_1 = \{\mathbf{y} = B_1\,\mathbf{x} \mid \mathbf{x} \in \mathbb{Z}^2\}. \tag{17}$$

III. EXHAUSTIVE SEARCH ALGORITHM

A. Overview

To find a gate V that satisfies Eq. (13), it behooves us to expand the Frobenius norm:

$$\begin{aligned}\left|\left|R^Z_{(0,1)}(\theta) - V\right|\right|^2 &= \sum_j \left(\sum_i \left|R^Z_{(0,1)}(\theta)_{ij} - V_{ij}\right|^2\right) \\ &= \sum_j \left|\left|R^Z_{(0,1)}(\theta)_j - V_j\right|\right|^2.\end{aligned} \tag{18}$$

From this, we see that the norm can be decomposed into a sum over column vectors; each contributes $\|R^Z_{(0,1)}(\theta)_i - V_i\|^2$. As a result, approximating $R^Z_{(0,1)}(\theta)$ may be reduced to approximating each of its column vectors with errors ε_i $(i = 1, 2, 3)$ such that $\sum_i \varepsilon_i^2 \leqslant \varepsilon^2$.

Consider a target unit vector $\mathbf{t}(j) = e^{i\alpha}\delta_{ij}$ with a single nonzero entry and α being a real number. To approximate it using a unit vector $\mathbf{v}$ imposes a condition on only one entry of $\mathbf{v}$:

$$\begin{aligned}\|\mathbf{t}(j) - \mathbf{v}\|^2 &= \sum_i |e^{i\alpha}\delta_{ij} - v_i|^2 \\ &= 2 - 2\ \mathrm{Re}(v_j\, e^{-i\alpha}).\end{aligned} \tag{19}$$

Requiring this to be bound by ε_j^2, we can apply it to Eq. (18) to give

$$\begin{aligned}&\mathrm{Re}\left(\frac{x_1}{\chi^f}e^{i\frac{\theta}{2}}\right) \geqslant \eta(\varepsilon_1), \quad \mathrm{Re}\left(\frac{y_2}{\chi^f}e^{-i\frac{\theta}{2}}\right) \geqslant \eta(\varepsilon_2), \\ &\mathrm{Re}\left(\frac{z_3}{\chi^f}\right) \geqslant \eta(\varepsilon_3),\end{aligned} \tag{20}$$

where $\eta(\varepsilon_i) := 1 - \varepsilon_i^2/2$.

To derive an algorithm, it is useful to further simplify Eq. (20). To do so, we note

$$\chi^{-f} = (-3)^{-f/2} = (-1)^{\lceil f/2\rceil} 3^{-\lceil f/2\rceil}\chi^{\bar{f}}, \tag{21}$$

where $\bar{f} := f \mod 2$. By introducing the change of variables

$$x_1' = (-1)^{\lceil f/2\rceil}\chi^{\bar{f}}x_1 \tag{22}$$

and applying similar transformations for y_2 and z_3, Eq. (20) can be rewritten as

$$\begin{aligned}\mathrm{Re}(x_1' e^{i\theta/2}) &\geqslant 3^{\lceil f/2\rceil}\eta(\varepsilon_1), \\ \mathrm{Re}(y_2' e^{-i\theta/2}) &\geqslant 3^{\lceil f/2\rceil}\eta(\varepsilon_2), \\ \mathrm{Re}(z_3') &\geqslant 3^{\lceil f/2\rceil}\eta(\varepsilon_3).\end{aligned} \tag{23}$$

[1] A localization of a ring R may be thought of as a method to introduce fractions.

[2] The Frobenius norm is $\|A\|_F^2 = \mathrm{tr}(A^\dagger A) = \sum_{i,j}|A_{ij}|^2$.

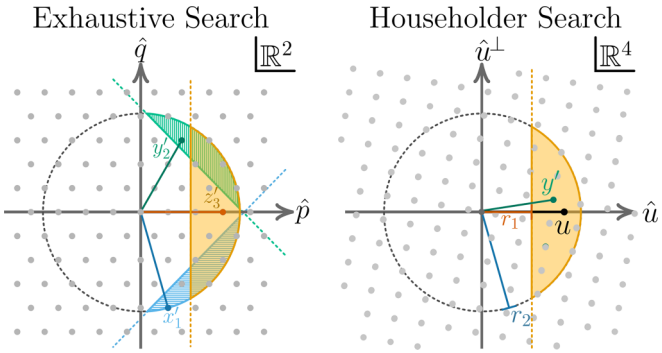

FIG. 1. Search regions for (left) exhaustive earch algorithm. The search regions of Eq. (23) are as follows: the blue corresponds to x_1', the green region corresponds to y_2', and the orange region corresponds to z_3'. (right) Householder search algorithm: $\mathbf{u} = \frac{1}{\sqrt{2}}(\cos\theta/2, \sin\theta/2, -1, 0)^T$. The yellow region corresponds to the search region in Eq. (50).

Moreover, the unitarity of V imposes the bounds

$$|x_1'|^2,\ |y_2'|^2,\ |z_3'|^2 \leqslant 3^{2\lceil f/2\rceil}. \tag{24}$$

The constraints of Eqs. 23 and 24 have straightforward geometric interpretations. That is, the Eisenstein integers x_1', y_2', and z_3' are lattice points in the respective shaded regions depicted in the left panel of Fig. 1.

Now, it is clear that the synthesis problem can be divided into two parts. The first part is to enumerate candidates' diagonal entries x_1, y_2, and z_3 satisfying Eqs. (20).

B. Enumeration of possible diagonal entries

This problem may be simply formulated as finding all the elements of a set

$$\mathcal{D}(\theta, f, \varepsilon) := \{x \in \mathcal{R}_3 \,|\, \mathrm{Re}(x/\chi^f) \leqslant \eta(\varepsilon) \text{and} |x/\chi^f| \leqslant 1\}. \tag{25}$$

where $f \in \mathbb{N}$ and $\eta(\varepsilon) := 1 - \varepsilon^2/2$. With this notation, for a fixed f, the diagonal entries x_1, y_2, and z_3 satisfy

$$x_1 \in \mathcal{D}(\theta, f, \varepsilon_1), \quad y_2 \in \mathcal{D}(-\theta, f, \varepsilon_2) \text{ and } z_3 \in \mathcal{D}(0, f, \varepsilon_3). \tag{26}$$

In fact, to satisfy $\varepsilon_1^2 + \varepsilon_2^2 + \varepsilon_3^2 \leqslant \varepsilon^2$, we may set $\varepsilon_1 = \varepsilon_2 = \varepsilon_3 = \varepsilon$ and exclude the triplets (x_1, y_2, z_3) for which Eq. (13) does not hold. Moreover, it is evident that

$$\mathcal{D}(-\theta, f, \varepsilon) = D^*(\theta, f, \varepsilon), \tag{27}$$

i.e., the set $\mathcal{D}(-\theta, f, \varepsilon)$ can be obtained by taking the complex conjugates of elements of $\mathcal{D}(\theta, f, \varepsilon)$. Therefore, to obtain candidates' diagonal entries x_1, y_2, and z_3 for a fixed f, it suffices to enumerate the sets $\mathcal{D}(\theta, f, \varepsilon)$ and $\mathcal{D}(0, f, \varepsilon)$. The enumeration algorithm is shown in Algorithm 1 and the full derivation is shown in Appendix A.

C. Unitary matrix completion

For a particular triplet $(x_1, y_2, z_3)/\chi^f$ for which Eq. (13) holds, the next step is to complete the unitary matrix, find the off-diagonal entries. To do so, we first check if the triplet satisfies the necessary and sufficient condition for a set of

ALGORITHM 1. Enumerate candidates (θ, f, ε).

Data: $\theta \in \mathbb{R}$, integer f, and precision ε.
Result: $\mathcal{D}(\theta, f, \varepsilon)$.

$\alpha \leftarrow -\frac{\theta}{2}$;
$\Gamma \leftarrow (-1)^{\lceil f/2\rceil}\chi^{\bar{f}}$;
$r_1 \leftarrow 3^{\lceil f/2\rceil}\eta(\varepsilon)$;
$r_2 \leftarrow 3^{\lceil f/2\rceil}$;
$S_\pm \leftarrow \frac{2}{\sqrt{3}}\left(r_1 \sin\alpha \pm \sqrt{r_2^2 - r_1^2\cos\alpha}\right)$;
$q \leftarrow \left\lceil \frac{S_-}{2} \right\rceil, \quad q_{\max} \leftarrow \left\lfloor \frac{S_+}{2} \right\rfloor$;
$\mathcal{D}(\theta, f, \varepsilon) \leftarrow$ empty list ;
while $q \leq q_{max}$ **do**
  $T_- \leftarrow \max\left(-\sqrt{r_2^2 - 3q^2}, \frac{r_1 - \sqrt{3}q\sin\alpha}{\cos\alpha}\right)$;
  $T_+ \leftarrow \sqrt{r_2^2 - 3q^2}$;
  $p \leftarrow \lceil 2T_- \rceil/2, \quad p_{\max} \leftarrow \lfloor 2T_+ \rfloor/2$;
  while $p \leq p_{max}$ **do**
    if $p + q \in \mathbb{Z}$ **then**
      $x' \leftarrow (p+q) + 2q\omega$;
      if γ *divides* x' **then**
        $x \leftarrow x'/\Gamma$;
        Insert x into $\mathcal{D}(\theta, f, \varepsilon)$;
    $p \leftarrow p + \frac{1}{2}$;
  $q \leftarrow q + \frac{1}{2}$;
return $\mathcal{D}(\theta, f, \varepsilon)$;

complex numbers to serve as the diagonal entries of a unitary matrix [91]. For $(\mathbf{C} + \mathbf{R})_3$ gates, these conditions are

$$|x_1| + |y_2| - |z_3| \leqslant \sqrt{3}^f, \quad |x_1| + |z_3| - |y_2| \leqslant \sqrt{3}^f,$$
$$|y_2| + |z_3| - |x_1| \leqslant \sqrt{3}^f. \tag{28}$$

For the triplets satisfying the conditions above, we proceed to finding the off-diagonal entries. In fact, the unitary matrix is determined (if one exists) once the lower triangular entries are found, see, i.e., Ref. [92]. Consequently, we search for entries x_2, x_3, and y_3.

We start by obtaining the entries x_2 and x_3. From unitarity, these entries satisfy

$$|x_1|^2 + |x_2|^2 + |x_3|^2 = 3^f. \tag{29}$$

Hence, they can be enumerated using an exhaustive search algorithm. That is, for every integer $0 \leqslant N \leqslant 3^f - |x_1|^2$, one uses Appendix C to find all solutions to the equation $|x_1|^2 = N$. If there exist such solutions, then one similarly proceeds to solving the equation $|x_3|^2 = 3^f - |x_1|^2 - N$.

Having obtained x_2 and x_3 from the discussion above, it remains to find candidates for y_3 to obtain the lower triangular matrix. Given that we have x_3 and y_2, the unitarity condition imposes

$$|y_3|^2 \leqslant \min(3^f - |x_3|^2, 3^f - |y_2|^2) \tag{30}$$

because both the rows and columns of a unitary matrix have unit norms. Then, we use the same enumeration method as in the case of x_2 to search for y_3 candidates.

Finally, once the lower triangular entries are specified, determining the upper triangular entries is straightforward. This can be done simply by determining whether there exist Eisenstein integers y_1, z_1, and z_2 consistent with unitarity. Equation (31) is a necessary condition (not sufficient) for the existence of y_1 and z_1 consistent with unitarity:

$$x_1^*|(x_2^* y_2 + x_3^* y_3) \text{ and } z_3^*|(x_2 x_3^* + y_2 y_3^*), \tag{31}$$

where for two Eisenstein integers a and b, $a|b$ means there exists another Eisenstein integer c such that $b = ac$. Determining if $a|b$ can be simply done by performing long division of b by a and $a|b$ is true if the remainder of the division is zero.

If the conditions in Eq. (31) hold, then the only candidates for y_1 and z_2 are given by

$$y_1 = -\frac{x_2^* y_2 + x_3^* y_3}{x_1^*} \quad \text{and} \quad z_2 = -\frac{x_2 x_3^* + y_2 y_3^*}{z_3^*}. \tag{32}$$

The last entry z_1 may be determined in several ways. A necessary condition for its existence consistent with unitarity is

$$x_1^*|(x_2^* z_2 + x_3^* z_3). \tag{33}$$

If this condition is satisfied, the only possible value is

$$z_1 = -\frac{x_2^* y_2 + x_3^* z_3}{x_1^*}. \tag{34}$$

With all the possible entries determined, it only remains to check $VV^\dagger = V^\dagger V = 1$, thus completing the algorithm. Algorithm 2 summarizes the `CompleteUnitary` subroutine and Algorithm 3 shows the full exhaustive search algorithm.

ALGORITHM 2. `CompleteUnitary`(x_1, y_2, z_3, f).

Data: $x_1, y_2, z_3 \in \mathcal{R}_3$ and $f \in \mathbb{N}$.
Result: Unitary matrix V.
if *x_1, y_2 and z_3 do not satisfy Eq. (28)* **then**
  return `Failure` ;
$N \leftarrow 0$;
while $N \leq 3^f - |x_1|^2$ **do**
  $S_{x_2} \leftarrow \{x_2 \in \mathcal{R}_3 : |x_2|^2 = N\}$;
  ; `// Use App. C to solve` $|x_2|^2 = N$
  foreach $x_2 \in S_{x_2}$ **do**
    $S_{x_3} \leftarrow \{x_3 \in \mathcal{R}_3 : |x_3|^2 = 3^f - |x_1|^2 - N\}$;
    $N' \leftarrow 0$;
    while $N' \leq \min(3^f - |x_3|^2,\ 3^f - |y_2|^2)$ **do**
      $S_{y_3} \leftarrow \{y_3 \in \mathcal{R}_3 : |y_3|^2 = N'\}$;
      foreach $y_3 \in S_{y_3}$ **do**
        if *Eq. (31) is true* **then**
          $y_1 \leftarrow -\frac{x_2^* y_2 + x_3^* y_3}{x_1^*}$;
          $z_2 \leftarrow -\frac{x_2 x_3^* + y_2 y_3^*}{z_3^*}$;
          if *Eq. (33) is true* **then**
            $z_1 \leftarrow -\frac{x_2^* y_2 + x_3^* z_3}{x_1^*}$;
            $V \leftarrow$ Eq. 11 ;
            if $VV^\dagger = V^\dagger V = 1$ **then**
              return V;
      $N' \leftarrow N' + 1$;
  $N \leftarrow N + 1$;
return `Failure`;

D. Time complexity

The time complexity can be split into two steps. Step (1) involves using Algorithm 1 to enumerate all valid triplets (x_1, y_2, z_3). The complexity of the enumeration algorithm (Algorithm 1) is determined by the area of each search region in Fig. 1. One can show that these areas are

$$3^{2\lceil f/2 \rceil} \varepsilon^2 \left(1 - \frac{\varepsilon^2}{4}\right) \arccos\left(1 - \frac{\varepsilon^2}{2}\right). \tag{35}$$

Expanding $\arccos(1 - \varepsilon^2/2) = \varepsilon + O(\varepsilon^3)$, we observe that this area scales as $O(3^f \varepsilon^3)$. Consequently, the total complexity of enumeration is $O(3^{3f} \varepsilon^9)$.

Step (2) of the algorithm is to complete the unitary (Algorithm 2). The complexity is dominated by solving Eq. (29) iteratively for $|x|^2 = N$ where $N = O(3^f \varepsilon^2)$. Which, in Appendix C, we showed leads to a complexity of $O(3^{f/2}\varepsilon)$.

Combining the complexity of both parts, we obtain $O(3^{7f/2}\varepsilon^{10})$ for a fixed f. The algorithm terminates at $f_{\max}$ once a solution is found. Recalling that we expect scaling $f_{\max} = c_1 \log \frac{1}{\varepsilon}$, the overall complexity is

$$\sum_{f=0}^{f_{\max}} 3^{\frac{7f}{2}} \varepsilon^{10} = O\left(3^{\frac{7}{2} f_{\max}} \varepsilon^{10}\right) = O\left(\varepsilon^{10 - \frac{7}{2} c_1}\right). \tag{36}$$

Finally, it is possible to derive a rough lower bound on c_1 by estimating the number of Eisenstein integers in each search region as follows: For a lattice $\mathcal{L}$ with basis $B = (\mathbf{b}_1, \mathbf{b}_2, \ldots, \mathbf{b}_m)$, the fundamental domain is

$$\mathcal{F}(\mathcal{L}) = \left\{ \sum_i c_i \mathbf{b}_i \,\middle|\, c_i \in \mathbb{R} \text{ and } c_i \in [0, 1) \right\}. \tag{37}$$

From Ref. [93], $\mathcal{L}$ is a uniform tiling of the ambient space with its fundamental domain. As a result, the volume of this domain is

$$\text{vol}(\mathcal{F}(\mathcal{L})) = \sqrt{\det(B^T B)}, \tag{38}$$

represents the inverse density of the lattice points. Therefore, the number of lattice points within a region, $\mathcal{K}$, of volume $\text{vol}(\mathcal{K})$ can be approximated by the ratio $\text{vol}(\mathcal{K})/\text{vol}(\mathcal{F}(\mathcal{L}))$.

For us, each search region has a $\text{vol}(\mathcal{K}) = O(3^f \varepsilon^3)$, and for $\mathcal{L}_1$, we find $\text{vol}(\mathcal{F}(\mathcal{L}_1)) = \sqrt{3}/2$. Requiring that at least one lattice point exists per volume then corresponds to

$$1 \leqslant \frac{\text{vol}(\mathcal{K})}{\text{vol}(\mathcal{F}(\mathcal{L}))} = \frac{3^f \varepsilon^3}{\sqrt{3}/2} = 2 \times 3^{c_1 \log_3 \frac{1}{\varepsilon} - \frac{1}{2}} \varepsilon^3. \tag{39}$$

Reducing this inequality yields $c_1 \geqslant 3$ and, consequently, $N_{\mathbf{R}} \geqslant 3 \log_3 \frac{1}{\varepsilon} + C$ where C is a constant.

IV. HOUSEHOLDER REFLECTION SEARCH

The poor scaling of the time complexity with ε of Algorithm 3 motivates us to search for more efficient ways to approximate diagonal gates. It was argued in Ref. [90] that by

ALGORITHM 3. Exhaustive search.

Data: θ and ε.
Result: $V \in U(3, \mathcal{R}_{3,\chi})$ such that $\|U - V\|_F \leq \varepsilon$.

$f \leftarrow 0$;
$\bar{f} \leftarrow f \bmod 2$;
$\Gamma \leftarrow (-1)^{\lceil f/2 \rceil} \chi^{\bar{f}}$;
while V *is not found* **do**
  $\mathcal{D}(0, f, \varepsilon) \leftarrow$ EnumerateCandidates$(0, f, \varepsilon)$;
  $\mathcal{D}(\theta, f, \varepsilon) \leftarrow$ EnumerateCandidates(θ, f, ε);
  $\mathcal{D}(-\theta, f, \varepsilon) \leftarrow \mathcal{D}(\theta, f, \varepsilon)^*$;
  foreach $x_1 \in \mathcal{D}(\theta, f, \varepsilon)$, $y_2 \in \mathcal{D}(-\theta, f, \varepsilon)$, $z_3 \in \mathcal{D}(0, f, \varepsilon)$ **do**
    $\varepsilon_1^2 \leftarrow 2 - 2\,\mathrm{Re}\left(x_1\, e^{i\theta/2}/\chi^f\right)$;
    $\varepsilon_2^2 \leftarrow 2 - 2\,\mathrm{Re}\left(y_2\, e^{-i\theta/2}/\chi^f\right)$;
    $\varepsilon_3^2 \leftarrow 2 - 2\,\mathrm{Re}\left(z_3/\chi^f\right)$;
    if $\varepsilon_1^2 + \varepsilon_2^2 + \varepsilon_3^2 \leq \varepsilon^2$ **then**
      $V \leftarrow$ CompleteUnitary(x_1, y_2, z_3, f) ;
      if V *is not* `Failure` **then**
        return V;
  $f \leftarrow f + 1$;
  $\bar{f} \leftarrow f \bmod 2$;
  $\Gamma \leftarrow (-1)^{\lceil f/2 \rceil} \chi^{\bar{f}}$;

restricting to Householder reflection of the form

$$R_{\mathbf{u}} = \mathbb{1} - 2\mathbf{u}\mathbf{u}^\dagger, \tag{40}$$

where $\mathbf{u}$ is a unit vector, there exists a probabilistic classical algorithm returning an approximation with average $N_R \sim 8 \log_3 \frac{1}{\varepsilon}$ using an average classical complexity $O(\log \frac{1}{\varepsilon})$. Further work in Ref. [79] reduced these estimates under certain number-theoretic conjectures to $N_R \sim 5 \log_3 \frac{1}{\varepsilon}$ for "nonexceptional" target two-level unit vectors. We present in these works an explicit algorithm and demonstrate its scaling for Householder reflections in the $(\mathbf{C} + \mathbf{R})_3$ group.

A. Overview

Reference [90] reformulated the approximation problem to only require approximating a unit vector $\mathbf{u} = (u_1, u_2, u_3)$ with another unit vector $\mathbf{v} = \frac{1}{\chi^f}(v_1, v_2, v_3)^T$ such that the entries $v_i \in \mathcal{R}_3$ and $f \in \mathbb{N}_0$.[3] We refer to such a unit vector as a unit Eisenstein vector. It is straightforward to verify that a $R^Z_{(0,1)}(\theta)$ matrix, up to a permutation, corresponds to a Householder reflection, i.e., $R^Z_{(0,1)}(\theta) = X_{(0,1)} R_{\mathbf{u}}$ for some

$$\mathbf{u} = \frac{1}{\sqrt{2}}(e^{i\theta/2}, -1, 0)^T. \tag{41}$$

We can derive an upper bound between two Householder reflections $R_{\mathbf{u}}$ and $R_{\mathbf{v}}$. To start, the norm between two Householder reflections can be related to their associated unit vectors

$$\|R_{\mathbf{u}} - R_{\mathbf{v}}\|^2 = 8(1 - |\mathbf{u}^\dagger \mathbf{v}|^2). \tag{42}$$

[3]This problem is related to the intrinsic Diophantine approximation [94].

Furthermore, for any two vectors $\mathbf{u}$ and $\mathbf{v}$

$$\|\mathbf{u} - \mathbf{v}\|^2 = 2[1 - \mathrm{Re}(\mathbf{u}^\dagger \mathbf{v})]. \tag{43}$$

Since, for any complex number z, the following inequality is true $(\mathrm{Re}[z])^2 \leqslant |z|^2$, combining with the previous expressions yields

$$\|R_{\mathbf{u}} - R_{\mathbf{v}}\| \leqslant 2\sqrt{2}\, \|\mathbf{u} - \mathbf{v}\|\, \delta(\mathbf{u}, \mathbf{v}), \tag{44}$$

where

$$\delta(\mathbf{u}, \mathbf{v}) := \sqrt{1 - \frac{\|\mathbf{u} - \mathbf{v}\|^2}{4}} \leqslant 1. \tag{45}$$

Using $\delta(\mathbf{u}, \mathbf{v}) \leqslant 1$ reproduces the bounds of Ref. [95], which demonstrates to approximate $R_{\mathbf{u}}$ within ε, it suffices to identify a $\mathbf{v}$ such that

$$||\mathbf{u} - \mathbf{v}|| \leqslant \varepsilon/(2\sqrt{2}). \tag{46}$$

However, given $\delta(\mathbf{u}, \mathbf{v}) \leqslant 1$ in Eq. (44) means that the requirement $\|\mathbf{u} - \mathbf{v}\| \leqslant \varepsilon/(2\sqrt{2})$ may exclude some $R_{\mathbf{v}}$ that meet the desired accuracy. To address this, we introduce into our algorithm a contraction factor $0 < c \leqslant 1$ and adjust the tolerance to $\varepsilon/(2\sqrt{2}\, c)$. While $c < 1$ no longer guarantees that all reflections remain within ε, those exceeding this threshold can be checked and rejected. This approach reduces $N_{\mathbf{R}}$ without increasing the algorithmic complexity, but the enlarged search space will lead in practice to longer run times.

From Eq. (41), we see that $u_3 = 0$. Thus, approximating $\mathbf{u}$ by $\mathbf{v} = \sqrt{-3}^{-f}(v_1, v_2, v_3)^T$ imposes the condition

$$\mathrm{Re}(u_1^* v_1' + u_2^* v_2') \geqslant r_1, \tag{47}$$

where we have rewritten terms using Eqs. (22) and (A1). Additionally, since $\mathbf{v}$ is a unit vector, it follows that

$$|v_1'| + |v_2'|^2 \leqslant r_2^2. \tag{48}$$

B. Geometric interpretation

These constraints on v_1' and v_2' have a straightforward formulation and geometric interpretation in $\mathbb{R}^4$. Any two-level complex vector $\mathbf{u} \in \mathbb{C}^3$ (with $u_3 = 0$ in our case) can be mapped to $\mathbb{R}^4$ by the isomorphism $\mathbf{u} = (u_1, u_2, 0)^T \mapsto \mathbf{u} = (\mathrm{Re}(u_1), \mathrm{Im}(u_1), \mathrm{Re}(u_2), \mathrm{Im}(u_2))^T$. By a slight abuse of notation, we refer to both the two-level complex and its image in $\mathbb{R}^4$ using the same letter. When the context does not make it obvious which version is being discussed, we clarify it explicitly.

In addition, consider for now the complex vector $(v_1, v_2)^T \in \mathbb{C}^2$ where $v_1, v_2 \in \mathcal{R}_3$. By defining these Eisenstein integers as $v_1 = x_1 + x_2\omega$ and $v_2 = x_3 + x_4\omega$ where $x_i \in \mathbb{Z}$, we can represent the complex vector $(v_1, v_2)^T$ in $\mathbb{R}^4$ by a vector $\mathbf{y} = (x_1 - \frac{x_2}{2}, \frac{\sqrt{3}}{2}x_2, x_3 - \frac{x_4}{2}, \frac{\sqrt{3}}{2}x_4)^T$. Consequently, it can be seen that the set of all such vectors $\mathbf{y}$ forms an integer lattice $\mathcal{L}_2$ in $\mathbb{R}^4$, defined by

$$\mathcal{L}_2 = \{\mathbf{y} = B_2\, \mathbf{x} | x \in \mathbb{Z}^4\}, \tag{49}$$

where $B_2 = B_1 \oplus B_1$ and B_1 are defined in Eq. (16). The Eisenstein integers v_1 and v_2 can be recovered from $\mathbf{y}$ via $\mathbf{x} = B_2^{-1}\mathbf{y}$.

To finally formulate the conditions in Eqs. (47) and (48) as vector constraints in $\mathbb{R}^4$, we denote the image of $(v_1', v_2')^T$ by a

lattice vector $\mathbf{y}' \in \mathcal{L}_2$. Then, these constraints can be rewritten as lattice points $\mathbf{y}'$ such that

$$\mathbf{u}^T\mathbf{y}' \geqslant r_1 \quad \text{and} \quad \mathbf{y}'^T\mathbf{y}' \leqslant r_2^2. \tag{50}$$

In other words, we are looking for lattice points $\mathbf{y}'$ above a hyperplane and inside a hypersphere of radius r_2, as demonstrated in Fig. 1. Denoting the volume between the hyperplane ($\mathbf{u}^T\mathbf{y}' = r_1$) and the hypersphere by $\mathcal{D}(\mathbf{u}, f, \varepsilon)$, we have $\mathbf{y}' \in \mathcal{L}_2 \cap \mathcal{D}(\mathbf{u}, f, \varepsilon)$.

Once such an Eisenstein vector $\mathbf{v} = \chi^{-f}(v_1, v_2, v_3)^T$ is found, the matrix $V = X_{(0,1)}R_{\mathbf{v}}$ is the desired approximation of $R^Z_{(0,1)}(\theta)$. It can be shown that synthesizing V requires $N_{\mathbf{R}} \leqslant 2f$ [76], and we provide a deterministic search algorithm focused on minimizing f.

Approximating V can thus be done in two iterated steps.

Step (1). Setting $\varepsilon' = \varepsilon/(2\sqrt{2}c)$, for a fixed $f \in \mathbb{N}_0$ and a unit vector $\mathbf{u} \in \mathbb{R}^4$, we enumerate all candidates $\mathbf{y}' \in \mathcal{L}_2 \cap \mathcal{D}(\mathbf{u}, f, \varepsilon')$ following the algorithm in Appendix B.

Step (2). For each $\mathbf{y}'$, we extract v_1 and v_2, and solve the norm equation $|v_3|^2 = 3^f - |v_1|^2 - |v_2|^2$, as discussed in Appendix C.

If a solution is found, we construct the vector $\mathbf{v}$ and subsequently the matrix $V = X_{(0,1)}R_{\mathbf{v}}$. It only remains to test that V approximates the target $R^Z_{(0,1)}(\theta)$ to the desired accuracy. Therefore, if $\|R^Z_{(0,1)}(\theta) - V\| \leqslant \varepsilon$, the matrix V is returned. In the event that all candidates $\mathbf{y}'$ are exhausted and no solution is found, we increment f and repeat the procedure. The details are summarized in Algorithm 4.

We now discuss the complexity of this algorithm. In Step (1), we enumerate all $\mathbf{y}'$ in the region bound by Eq. (50). For a fixed f, the complexity of this corresponds to the volume of the region. Due to spherical symmetry, this volume corresponds to that of a hyperspherical cap in $\mathbb{R}^4$ defined by the constraints $y_4 \geqslant r_1$ and $\mathbf{y}^T\mathbf{y} \leqslant r_2^2$. According to Ref. [96], this volume is given by

$$\text{vol}\left(\mathcal{D}(\mathbf{u}, f, \varepsilon)\right) = \frac{\pi^{3/2}}{\Gamma(5/2)} r_2^4 \int_0^{\phi} \sin^4\theta \, d\theta, \tag{51}$$

where $\phi = \arccos(r_1/r_2) = \arccos(1 - \varepsilon^2/2)$. Evaluating this integral yields:

$$\begin{aligned}\text{vol}\left(\mathcal{D}(\mathbf{u}, f, \varepsilon)\right) &= \frac{\pi r_2^4}{24}[12\phi - 8\sin(2\phi) + \sin(4\phi)] \\ &= \frac{4\pi}{15} r_2^4 \varepsilon^5 + O\big(r_2^4\varepsilon^7\big),\end{aligned} \tag{52}$$

where we expanded in the $\varepsilon \to 0$ limit. Using the definition of r_2 in Eq. (A1) gives us a final scaling for Step (1) of $O(3^{2f}\varepsilon^5)$.

The problem in Step (2) is to solve the norm equation in Eq. (48) using the exhaustive search method in Appendix C, which has complexity $O(|v_3|)$. We show in Appendix D that $|v_3| = O(3^{f/2}\varepsilon)$. Combining these two steps, the complexity of the Householder search method is $O(3^{5f/2}\varepsilon^6)$. Similarly to the exhaustive algorithm, this one terminates at $f_{\max}$. Assuming the scaling $f_{\max} = c_2 \log \frac{1}{\varepsilon}$, the overall

$$\sum_{f=0}^{f_{\max}} 3^{\frac{5}{2}f}\varepsilon^6 = O\big(3^{\frac{5}{2}f_{\max}}\varepsilon^6\big) = O\big(\varepsilon^{6-\frac{5}{2}c_2}\big). \tag{53}$$

Similarly, it is also possible to place a rough lower bound on c_2. The volume of the search region in Fig. 1 (right) is $O(3^{2f}\varepsilon^5)$. Using the arguments at the end of Sec. III, we obtain $c_2 \geqslant 2.5$. This lower bound corresponds to $N_{\mathbf{R}} \geqslant 5\log_3\frac{1}{\varepsilon} + C$ where C is a constant.

ALGORITHM 4. Householder reflection search.

Data: θ, ε, and $0 < c \leq 1$.
Result: $V \in U(3, \mathcal{R}_{3,\chi})$ such that $\|U - V\|_F \leq \varepsilon$.

$\mathbf{u} \leftarrow \frac{1}{\sqrt{2}}(\cos\theta/2, \sin\theta/2, -1, 0)^T$;
$\varepsilon' \leftarrow \varepsilon/(2\sqrt{2}c)$;
$f \leftarrow 0$;
$\bar{f} \leftarrow f \bmod 2$
$\Gamma \leftarrow (-1)^{\lceil f/2 \rceil}\chi^{\bar{f}}$;
while $\mathbf{v}$ *is not found* **do**
  foreach $\mathbf{y}'$ *in* $\mathcal{L}_2 \cap \mathcal{D}(\mathbf{u}, f, \varepsilon')$ **do**
    $\mathbf{x}' \leftarrow B_2^{-1}\mathbf{y}'$;
    $v_1' \leftarrow x_1' + x_2'\omega$ and $v_2' \leftarrow x_3' + x_4'\omega$;
    if Γ *divides* v_1' *and* Γ *divides* v_2' **then**
      $v_1 \leftarrow v_1'/\Gamma$ and $v_2 \leftarrow v_2'/\Gamma$;
      $S_{v_3} \leftarrow \{v_3 \in \mathcal{R} : |v_3|^2 = 3^f - |v_1|^2 - |v_2|^2\}$
      foreach $v_3 \in S_{v_3}$ **do**
        $\mathbf{v} \leftarrow \frac{1}{\chi^f}(v_1, v_2, v_3)^T$;
        $V \leftarrow X_{(0,1)}R_{\mathbf{v}}$;
        if $\|R^Z_{(0,1)}(\theta) - V\| \leq \varepsilon$ **then**
          return V ;
  $f \leftarrow f + 1$;
  $\bar{f} \leftarrow f \bmod 2$;
  $\Gamma \leftarrow (-1)^{\lceil f/2 \rceil}\chi^{\bar{f}}$;

V. EXACT SYNTHESIS

Given the approximation gate $V \in U(3, \mathcal{R}_{3,\chi})$, what remains is to determine the word in $(\mathbf{C} + \mathbf{T})_3$ which produces it. To do this, one uses the fact that any V can be written optimally in a normal form [76]:

$$V = \prod_i^f HD(a_{0,i}, a_{1,i}, a_{2,i})\mathbf{R}^{\varepsilon_i}X^{\delta_i}, \tag{54}$$

where $a_{0,i}, a_{1,i}, a_{2,i}, \delta_i \in \{0, 1, 2\}$, and $\varepsilon_i \in \{0, 1\}$. While this form is more complicated than the analogous normal form for qubits [97] that contain only H, T, S, there is still only one non-Clifford gate, $\mathbf{R}$, since $D(a, b, c)$ and X can be constructed from H, S as shown above. Taken together, the total number of possible normal forms N_N smaller than f is

$$N_N = \sum_{i=0}^{f}(3^4 2^2)^i = \frac{324^{f+1} - 1}{323}. \tag{55}$$

To determine the correct normal form, and therefore circuit, we implement the algorithm from Ref. [76], which guarantees optimality in $N_{\mathbf{R}}$.

To do this, we take advantage of the *smallest denominator exponent* $\text{sde}(z)$ which corresponds to the smallest non-negative integer f such that $z\chi^f \in \mathcal{R}_3$ when $z \in \mathcal{R}_{3,\chi}$. It was shown in Ref. [76] that all entries of a matrix in

ALGORITHM 5. Decomposition of V in $U(3, \mathcal{R}_{3,\chi})$.

Data: Unitary U in $U(3, \mathcal{R}_{3,\chi})$.
T_D - table of all zero-sde unitaries in $U(3, \mathcal{R}_{3,\chi})$.
Result: Sequence S_{out} of $H, D, \mathbf{R}$, and X gates that implement U.

$u \leftarrow$ top left entry of U;
$S_{\text{out}} \leftarrow$ Empty;
$s \leftarrow \text{sde}(u)$;
while $s > 0$ **do**
  state $\leftarrow$ unfound;
  forall $a_0, a_1, a_2, \delta \in \{0, 1, 2\}, \varepsilon \in \{0, 1\}$ **do**
    while *state* = *unfound* **do**
      $u \leftarrow (HD(a_0, a_1, a_2)\mathbf{R}^{\varepsilon}X^{\delta}U)_{00}$;
      if $\text{sde}(u) = s - 1$ **then**
        state $\leftarrow$ found;
        append $X^{-\delta}\mathbf{R}^{-\varepsilon}D^{-1}H$ to S_{out};
        $s \leftarrow \text{sde}(u)$;
        $U \leftarrow HD(a_0, a_1, a_2)\mathbf{R}^{\varepsilon}X^{\delta}U$;
lookup matrix S_{rem} for U in T_D;
append S_{rem} to S_{out};
return S_{out};

$U(3, \mathcal{R}_{3,\chi})$ have the same $\text{sde}(z)$. Therefore, an algorithm for solving Eq. (54) is to iteratively find a set $a_{0,i}, a_{1,i}, a_{2,i}, \delta_i, \varepsilon_i$ that reduces the $\text{sde}(z)$ by 1. Each reduction corresponds to at most one $\mathbf{R}$ gate per iteration. Once $\text{sde}(z) = 0$, the resulting unitary can then be obtained from a lookup table. The pseudocode is detailed in Algorithm 5.

VI. NUMERICAL RESULTS

We now discuss the numerical results for our work and compare them to existing methods, including Bocharov *et al.* [79]. And the asymptotic theoretical upper bounds expected from these algorithms. We provide the scaling for the $N_{\mathbf{R}}$ compared with the infidelity, ε in Fig. 2. For both algorithms, we investigated the statistical distribution of $N_{\mathcal{G}}$ for a random sample of up to 10^4 angles and found that the cost is strongly peaked and nearly normally distributed. Therefore, for our numerical results, we restricted ourselves to 100 random angles between $(-\pi/2, \pi/2)$. Using the exhaustive algorithm, we evaluated angles at 10 target precisions $\varepsilon \in \{1, 0.5, 0.25, 0.1, \ldots, 10^{-3}\}$. From this, we find on average

$$N_{\mathbf{R}}^{E}(\varepsilon) = 2.193(11) + 8.621(7)\log_{10}(1/\varepsilon) = 2.193(11) + 4.113(3)\log_3(1/\varepsilon). \quad (56)$$

For the Householder search algorithm, we evaluated angles at 11 target precisions $\varepsilon \in \{1, 10^{-1}, \ldots, 10^{-10}\}$. After a modest search through contraction factors, we found that $c = 0.35$ yields short word lengths with tolerable additional runtime. Using this faster algorithm gave

$$N_{\mathbf{R}}^{H}(\varepsilon) = 3.20(13) + 10.77(3)\log_{10}(1/\varepsilon) = 3.20(13) + 5.139(14)\log_3(1/\varepsilon). \quad (57)$$

We can use the average costs [Eqs. (57) and (56)], along with Eqs. (36) and (53), to compute the average complexity of both algorithms. For the full $(\mathbf{C} + \mathbf{R})_3$ search, the average c_1 corresponds to the slope 4.11, which yields an average complexity of $O(\varepsilon^{-4.4})$. In the case of the Householder search, the average c_2 is half the slope, 5.139, resulting in an average complexity of $O(\varepsilon^{-0.42})$.

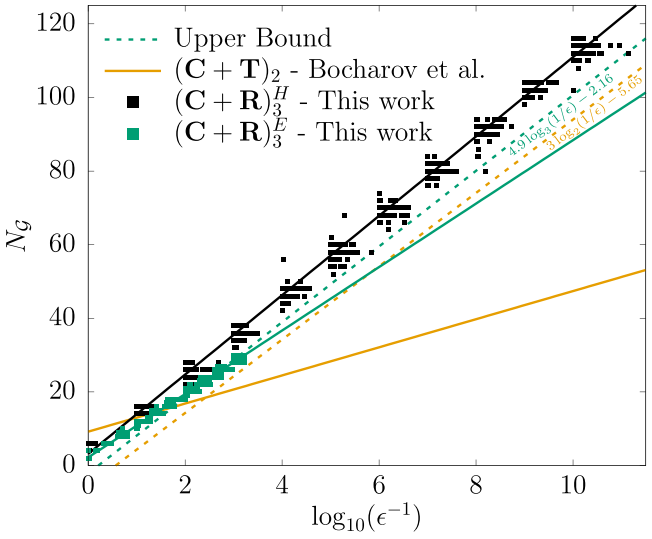

FIG. 2. Scaling of the number of non-Clifford gates $N_{\mathcal{G}}$ ($\mathbf{T}$ or $\mathbf{R}$ depending on qudit dimension) against the infidelity ε. Angles are uniformly sampled in the region $\theta \in (-\pi/2, \pi/2)$. The work of Bocharov *et al.* [79] for qubits is shown with the orange line. The black data points and solid black line correspond to our qutrit Householder algorithm and fit. The green squares and solid green line are our qutrit exhaustive algorithm and fit. The dashed lines correspond to theoretical asymptotic upper bounds.

To determine the average cost for an arbitrary single-qutrit SU(3) gate, these results should be multiplied by 6 [79]. Given the importance of the $\mathbf{T}_3$ gate in discussions of qutrits, we investigate its approximate synthesis with the Householder search algorithm, finding N_R^H for $\mathbf{T}_3$ aligns with that of the average gate costs. In passing, we also note that $N_{\mathbf{R}}$ exhibits a weak angular dependence: angles closer to $R_{3,\chi}$ lead to lower $N_{\mathbf{R}}$.

With these results, we can compare our single-qutrit synthesis method to that of implementing the same unitary on two qubits. For the general case of two-qubit circuits with cnots and $R^{\alpha}(\theta)$, i.e., SU(4), 15 single-qubit rotations are required [98]. Restricting to the single-qutrit subspace of SU(3), dimensional analysis bounds the cost as at least 10 $R^{\alpha}(\theta)$. Using the average cost for synthesizing $R^Z(\theta)$ from [89] of $N_T^{RUS} = 9.2 + 3.817\log_{10}(1/\varepsilon) = 9.2 + 1.15\log_2(1/\varepsilon)$ would estimate that an arbitrary single-qutrit gate would require at least 10 N_T^{RUS}. Comparing with the costs in Eqs. (56) and (57) imply that single-qutrit synthesis via our algorithms for $\mathbf{R}$ incurs an overhead factor as $\varepsilon \to 0$ of 1.35 and 1.69, respectively. If one instead considers a fiducial $\varepsilon = 10^{-10}$, these factors reduce to 1.12 and 1.40, respectively.

VII. EXAMPLE APPLICATION

It is important to provide context for how some of these results compare with application-specific problems. For

example, a prototypical quantum Hamiltonian in high-energy physics can be truncated to a three-level system that is mappable to qutrits [48,99,100]. In these models, the unitary evolution of three different types of terms needs to be implemented:

$$e^{-itU^x},\ e^{-itL^z},\quad \text{and}\quad e^{-itL^z\otimes L^z}, \tag{58}$$

where

$$U^x = \frac{1}{\sqrt{2}}\begin{pmatrix}0&1&0\\1&0&1\\0&1&0\end{pmatrix}\quad\text{and}\quad L^z = \begin{pmatrix}1&0&0\\0&0&0\\0&0&-1\end{pmatrix}. \tag{59}$$

One of the authors provided quantum circuits to construct these operators in Refs. [48,101]. The $L^z \otimes L^z$ rotation requires eight R^Z rotations for qubits to be synthesized, while only requiring four for qutrits. This leads to a qubit-based cost of synthesis of

$$N_T^{RUS}(L^z \otimes L^z) = 73.6 + 30.536\log_{10}(1/\varepsilon) \tag{60}$$

while the qutrit-based implementation, depending on the synthesis algorithm, only requires

$$N_{\mathbf{R}}^{H}(L^z \otimes L^z) = 12.80(52) + 43.08(12)\log_{10}(1/\varepsilon) \tag{61}$$

or

$$N_{\mathbf{R}}^{E}(L^z \otimes L^z) = 8.772(448) + 34.484(28)\log_{10}(1/\varepsilon). \tag{62}$$

Therefore, $N_{\mathcal{G}}$ for a qutrit implementation is smaller than Bocharov *et al.*'s repeat-until-success method for synthesis errors of $\varepsilon > 10^{-17}$ for an exhaustive search, and for $\varepsilon > 10^{-5}$ for the Householder algorithm.

Meanwhile, the operator U^x can be broken up into 1 $R^Z_{(a,b)}$ rotations that need to be synthesized. This would be compared with the 5 qubit R^Z rotations. This leads to the qubit implementation requiring

$$N_T^{RUS}(U^x) = 46 + 19.09\log_{10}(1/\varepsilon), \tag{63}$$

while the qutrit ones scale as

$$\begin{aligned} N_{\mathbf{R}}^{E}(U^x) &= 2.193(11) + 8.621(7)\log_{10}(1/\varepsilon),\\ N_{\mathbf{R}}^{H}(U^x) &= 3.20(13) + 10.77(3)\log_{10}(1/\varepsilon). \end{aligned} \tag{64}$$

In this case, both qutrit implementations are strictly superior to the qubit RUS implementation. Taken together, this suggests that a fault-tolerant implementation of this high-energy physics model could be performed more efficiently in terms of non-Clifford gates with qutrits for reasonable ranges of ϵ.

VIII. CONCLUSION

In this work, we have demonstrated algorithms to synthesize diagonal gates for qutrits using the Clifford + **R** gates. Our studies show that given a target infidelity ε for a diagonal rotation gate, one can approximate a diagonal that requires approximately $3.20(13) + 10.77(3)\log_{10}(1/\varepsilon)$ **R** gates. These results open up the feasibility of using fault-tolerant qutrits for quantum simulations. While these results are valuable, they leave several open questions. First, while the prefactor 10.77(3) for synthesizing diagonal gates is close to the lower bound of 10.27, multiplying by six to obtain arbitrary gates leaves us quite far from optimality. Potential improvements could come from exploring repeat-until-success methods [89] or identifying broader subclasses of gates that can be efficiently synthesized. Another direction of research might investigate synthesis with other groups, such as $(\mathbf{C}+\mathbf{D})_3$ or $(\mathbf{C}+\mathbf{T})_3$. Furthermore, similar to qubits, looking for larger transverse groups than Cliffords could further reduce the cost [69,70] and potentially enable novel application-specific gate sets, i.e., high-energy physics [55,102].

ACKNOWLEDGMENTS

The authors thank Namit Anand, Michael Cervia, Di Fang, Yao Ji, Aaron Lott, and Yu Tong for their helpful comments and suggestions. This material is based on work supported by the U.S. Department of Energy, Office of Science, National Quantum Information Science Research Centers, Superconducting Quantum Materials and Systems Center (SQMS) under Contract No. DE-AC02-07CH11359. This work was produced by Fermi Forward Discovery Group, LLC under Contract No. 89243024CSC000002 with the U.S. Department of Energy, Office of Science, Office of High Energy Physics. E.G. was supported by the NASA Academic Mission Services, Contract No. NNA16BD14C and the Intelligent Systems Research and Development-3 (ISRDS-3) Contract No. 80ARC020D0010 under the NASA-DOE interagency agreement SAA2-403602. E.M. acknowledges support from the US Department of Energy, Office of Science, Nuclear Physics, under the Grant No. DE-FG02-95ER40907. S.Z. acknowledges support from the US Department of Energy, Office of Science, Accelerated Research in Quantum Computing Centers, Quantum Utility through Advanced Computational Quantum Algorithms, Grant No. DE-SC0025572. D.L. acknowledges support from DMREF Award No. 1922165, Simons Targeted Grant Award No. 896630, and a Willard Miller Jr. Fellowship.

DATA AVAILABILITY

The data that support the findings of this article are not publicly available because of legal restrictions preventing unrestricted public distribution. The data are available from the authors upon reasonable request.

APPENDIX A: ENUMERATION ALGORITHM

From Equations (17) and (16), we find that it is convenient to work with a half-integer parametrization (p, q). That is, for an Eisenstein integer $x_1 + x_2\omega$, we set $p = x_1 - x_2/2$ and $q = x_2/2$. Thus satisfying Eqs. (23) and (24) corresponds to finding three lattice vectors $(p, q\sqrt{3})^T$ each in a different region. Using α to represent the desired angles and

$$r_1 = 3^{\lceil f/2\rceil}\eta(\varepsilon_i),\quad r_2 = 3^{\lceil f/2\rceil}, \tag{A1}$$

the three regions are then defined by

$$p\cos\alpha + q\sqrt{3}\sin\alpha \geqslant r_1 \text{ and } p^2 + 3q^2 \leqslant r_2^2. \tag{A2}$$

From the first inequality, it follows that $p^2\cos^2\alpha \geqslant (r_1 - q\sqrt{3}\sin\alpha)^2$. Using the second constraint and completing the square, it can be verified that $|\sqrt{3}q - r_1\sin\alpha| \leqslant (r_2^2 - r_1^2)^{1/2}\cos\alpha$. There-

fore, the half-integers q are sampled within the interval

$$\tfrac{1}{2}\lceil S_- \rceil \leqslant q \leqslant \tfrac{1}{2}\lfloor S_+ \rfloor, \tag{A3}$$

where $S_\pm := \frac{2}{\sqrt{3}}[r_1 \sin\alpha \pm (r_2^2 - r_1^2)^{1/2}\cos\alpha]$. For a given q, the possible values of p satisfy $p + q \in \mathbb{Z}$ and lie in the interval

$$\tfrac{1}{2}\lceil 2T_- \rceil \leqslant p \leqslant \tfrac{1}{2}\lfloor 2T_+ \rfloor, \tag{A4}$$

where $T_- := \max[-(r_2^2 - 3q^2)^{1/2}, \frac{r_1 - \sqrt{3}q\sin\alpha}{\cos\alpha}]$ and $T_+ := (r_2^2 - 3q^2)^{1/2}$.

APPENDIX B: ENUMERATION ALGORITHM FOR $\mathbf{y} \in \mathcal{L}_2 \cap \mathcal{D}(\mathbf{u}, f, \varepsilon)$

The goal is to enumerate all vectors $\mathbf{y} \in \mathcal{L}_2 \cap \mathcal{D}(\mathbf{u}, f, \varepsilon)$ for a fixed $f \geqslant 0$. As defined in Eq. (49), the lattice vectors $\mathbf{y} \in \mathcal{L}_2$ take the form $\mathbf{y} = B_2\mathbf{x}$, where $\mathbf{x} \in \mathbb{Z}^4$. By matrix multiplication, $\mathbf{y}$ can be written as

$$\mathbf{y} = \left(x_1 - \frac{x_2}{2}, \frac{\sqrt{3}}{2}x_2, x_3 - \frac{x_4}{2}, \frac{\sqrt{3}}{2}x_4\right)^T. \tag{B1}$$

It is convenient to parametrize $\mathbf{y}$ with half-integers p_1, q_1, p_2, q_2 such that $p_i := x_i - x_{2i}/2$ and $q_i := x_{2i}/2$ where $i = 1, 2$. Each pair (p_i, q_i) must satisfy the integer constraint $x_i = p_i + q_i$. Consequently, the lattice vectors take the form $\mathbf{y} = (p_1, \sqrt{3}q_1, p_2, \sqrt{3}q_2)^T$ and $\mathbf{y}^T\mathbf{y} = \sum_{i=1}^2 p_i^2 + 3q_i^2$.

Lemma B 1. For $\mathbf{y} \in \mathcal{D}(\mathbf{u}, f, \varepsilon)$, $|y_4| \leqslant (r_2^2 - r_1^2)^{1/2}$.

Proof. Let $\mathbf{e}_i$ (with $i = 1, 2, 3, 4$) be the canonical basis vectors of $\mathbb{R}^4$. That is, $\mathbf{e}_1 = (1, 0, 0, 0)^T$. Let Π_3 be the projector onto the subspace spanned by $\mathbf{e}_1, \mathbf{e}_2$, and $\mathbf{e}_3$. Since $u_4 = 0$, it follows that $\mathbf{u}^T\mathbf{y} = \mathbf{u}^T\Pi_3\mathbf{y}$. By the triangle inequality, $(\Pi_3\mathbf{y})^T(\Pi_3\mathbf{y}) \geqslant r_1^2$. Additionally, using the total norm constraint: $\mathbf{y}^T\mathbf{y} = (\Pi_3\mathbf{y})^T(\Pi_3\mathbf{y}) + y_4^2 \leqslant r_2^2$, implying that $y_4^2 \leqslant r_2^2 - r_1^2$ or, equivalently, $|y_4| \leqslant (r_2^2 - r_1^2)^{1/2}$. ∎

This lemma constrains the sampling range for q_2:

$$\frac{1}{2}\left\lceil -2\sqrt{\frac{r_2^2 - r_1^2}{3}} \right\rceil \leqslant q_2 \leqslant \frac{1}{2}\left\lfloor 2\sqrt{\frac{r_2^2 - r_1^2}{3}} \right\rfloor. \tag{B2}$$

For each q_2, the other components satisfy:

$$\begin{aligned} q_1\cos(\alpha) + \sqrt{3}q_1\sin(\alpha) &\geqslant \sqrt{2}r_1 + p_2, \\ q_1^2 + 3q_1^2 &\leqslant r_2^2 - 3q_2^2 - p_2^2, \end{aligned} \tag{B3}$$

where $\alpha := \theta/2$. Since $(\cos\alpha, \sin\alpha)^T$ is a unit vector, applying the arguments in Lemma B 1 gives

$$|\sqrt{2}r_1 + p_2| \leqslant \sqrt{r_2^2 - 3q_2^2 - p_2^2}. \tag{B4}$$

This inequality holds only for p_2 within the interval:

$$\tfrac{1}{2}\lceil 2\,p_{2,\min} \rceil \leqslant p_2 \leqslant \tfrac{1}{2}\lfloor 2\,p_{2,\max} \rfloor, \tag{B5}$$

where $p_{2,(\max,\min)} := \frac{1}{\sqrt{2}}[-r_1 \pm (r_2^2 - r_1^2 - 3q_2^2)^{1/2}]$. Note that ensuring that the radicand is non-negative provides an elementary proof of Lemma B 1. With p_2 and q_2 determined, Eq. (B3) can be rewritten as

$$p_1\cos(\alpha) + \sqrt{3}q_1\sin(\alpha) \geqslant \lambda_1, \quad p_1^2 + 3q_1^2 \leqslant \lambda_2^2, \tag{B6}$$

with $\lambda_1 := \sqrt{2}r_1 + p_2$ and $\lambda_2^2 := r_2^2 - 3q_2^2 - p_2^2$. Enumerating such p_1 and q_1 can be done using the results in Eqs. (A3) and (A4).

APPENDIX C: SOLVING THE NORM EQUATION

This Appendix describes how to solve the norm equation. Specifically, given a positive integer N, the problem is to find an Eisenstein integer $x = a + b\omega$ such that $|x|^2 = N$. Using the half-integer representation, $p = a - \frac{b}{2}$, $q = \frac{b}{2}$, the norm equation can be rearranged to

$$p^2 + 3q^2 - N = 0. \tag{C1}$$

Interpreting this as a quadratic equation in p, the discriminant is given by $\Delta = 4N - 12q^2$. Real solutions for p exist if $\Delta \geqslant 0$, which requires $q^2 \leqslant N/3$. Hence, valid values of q are half-integers satisfying $|q| \leqslant \lfloor\sqrt{N/3}\rfloor$.

Since the equation is symmetric under $q \to -q$, it suffices to consider only non-negative values of q. For each q, if $p = \pm(N - 3q^2)^{1/2}$ such that $p + q \in \mathbb{Z}$, then a valid solution exists. Together, this gives an $x = (p + q) + (2q)\omega$ which satisfies the norm equation. Finally, the complexity of this search is $O(\sqrt{N})$.

It is important to note that because the norm of Eisenstein integers is multiplicative:

$$\left|\prod_i x_i\right|^2 = \prod_i |x_i|^2 \quad \text{for} \quad x_i \in \mathcal{R}_3. \tag{C2}$$

The norm equation $|x|^2 = N$ for $\in \mathcal{R}_3$ can be solved with a factoring algorithm. Given an integer factorization $N = \prod_i p_i^{c_i}$, there is a method to solve $|x|^2 = N$ which relies on the relation between rational primes and Eisenstein primes, see, e.g., Ref. [103]. Indeed, a rational prime $p \neq 3$ either remains prime in $\mathcal{R}_3$ or splits in $\mathcal{R}_3$. That is, if $p \in \mathbb{Z}$ is prime, then p is also prime in $\mathcal{R}_3$ if $p \equiv 2 \pmod 3$. On the other hand, if $p \equiv 1 \pmod 3$, there exists $\eta \in \mathcal{R}_3$ such that $|\eta|^2 = p$. In the case $p = 3$, $|1 - \omega|^2 = 3$.

Then, having the factorization for N, solving $|x|^2 = N$ reduces to solving each $|x_i|^2 = p_i$ for the case $p_i \equiv 1 \pmod 3$.[4] This can be solved using the method described earlier with complexity only $O(\sqrt{p_i})$. However, integer factorization using a general number field sieve (GNFS) algorithm [104] would reduce the complexity.

APPENDIX D: BOUND ON $|v_3|$

As shown in Appendix C, the complexity of finding v_3 via exhaustive search depends on $|v_3|$. This section establishes an upper bound on this value. For all $\mathbf{y}' \in \mathcal{L}_2 \cap \mathcal{D}(\mathbf{u}, f, \varepsilon)$, the triangle inequality implies $|\mathbf{u}^T\mathbf{y}'| \leqslant |\mathbf{y}'|$, which can be used to show $\mathbf{y}'^T\mathbf{y}' \geqslant r_1^2$.

[4] For $p_i = 3$, $x_i = 1 - \omega$. For $p_i \equiv 2 \bmod 3$, $x_i = p_i^{c_i/2}$ if and only if c_i is even because such p_i is prime in $\mathcal{R}_3$.

For Eisenstein $\mathbf{y}'$, it follows that $\mathbf{y}'^T\mathbf{y}' = |v'_1|^2 + |v'_2|^2 \leqslant r_2^2$. Applying the variable change of Eq. (22), we obtain

$$|v_1|^2 + |v_2|^2 \geqslant 3^{-\bar{f}} r_1^2. \tag{D1}$$

Remembering that $|v_3|^2 = 3^f - (|v_1|^2 + |v_2|^2)$, this equation simplifies by noting that $3^{2\lceil f/2\rceil - \bar{f}} = 3^f$ to yield

$$|v_3| \leqslant 3^{f/2}\varepsilon\sqrt{1-\varepsilon^2/4} = O(3^{f/2}\varepsilon). \tag{D2}$$

[1] M. Ringbauer, M. Meth, L. Postler, R. Stricker, R. Blatt, P. Schindler, and T. Monz, A universal qudit quantum processor with trapped ions, Nat. Phys. **18**, 1053 (2022).

[2] P. J. Low, B. White, and C. Senko, Control and readout of a 13-level trapped ion qudit, npj Quantum Inf. **11**, 85 (2025).

[3] A. S. Nikolaeva *et al.*, Scalable improvement of the generalized Toffoli gate realization using trapped-ion-based qutrits, Phys. Rev. Lett. **135**, 060601 (2025).

[4] A. Galda, M. Cubeddu, N. Kanazawa, P. Narang, and N. Earnest-Noble, Implementing a ternary decomposition of the Toffoli gate on fixed-frequency transmon qutrits, arXiv:2109.00558.

[5] N. Goss *et al.*, High-fidelity qutrit entangling gates for superconducting circuits, Nat. Commun. **13**, 7481 (2022); **14**, 4256(E) (2023).

[6] K. Luo *et al.*, Experimental realization of two qutrits gate with tunable coupling in superconducting circuits, Phys. Rev. Lett. **130**, 030603 (2023).

[7] L. E. Fischer, A. Chiesa, F. Tacchino, D. J. Egger, S. Carretta, and I. Tavernelli, Universal qudit gate synthesis for transmons, PRX Quantum **4**, 030327 (2023).

[8] N. Goss, S. Ferracin, A. Hashim, A. Carignan-Dugas, J. M. Kreikebaum, R. K. Naik, D. I. Santiago, and I. Siddiqi, Extending the computational reach of a superconducting qutrit processor, npj Quantum Inf. **10**, 101 (2024).

[9] S. Cao, M. Bakr, G. Campanaro, S. D. Fasciati, J. Wills, D. Lall, B. Shteynas, V. Chidambaram, I. Rungger, and P. Leek, Emulating two qubits with a four-level transmon qudit for variational quantum algorithms, Quantum Sci. Technol. **9**, 035003 (2024).

[10] L. M. Seifert, Z. Li, T. Roy, D. I. Schuster, F. T. Chong, and J. M. Baker, Exploring ququart computation on a transmon using optimal control, Phys. Rev. A **108**, 062609 (2023).

[11] Y. Iiyama, W. Jang, N. Kanazawa, R. Sawada, T. Onodera, and K. Terashi, Qudit-generalization of the qubit echo and its application to a qutrit-based Toffoli gate, arXiv:2405.14752.

[12] Z. Wang, R. W. Parker, E. Champion, and M. S. Blok, Systematic study of high E_J/E_C transmon qudits up to $d = 12$, Phys. Rev. Appl. **23**, 034046 (2025).

[13] A. Kruckenhauser, R. van Bijnen, T. V. Zache, M. Di Liberto, and P. Zoller, High-dimensional SO(4)-symmetric Rydberg manifolds for quantum simulation, Quantum Sci. Technol. **8**, 015020 (2023).

[14] S. R. Cohen and J. D. Thompson, Quantum computing with circular Rydberg atoms, PRX Quantum **2**, 030322 (2021).

[15] Y. Chi *et al.*, A programmable qudit-based quantum processor, Nat. Commun. **13**, 1166 (2022).

[16] V. Kasper, D. González-Cuadra, A. Hegde, A. Xia, A. Dauphin, F. Huber, E. Tiemann, M. Lewenstein, F. Jendrzejewski, and P. Hauke, Universal quantum computation and quantum error correction with ultracold atomic mixtures, Quantum Sci. Technol. **7**, 015008 (2022).

[17] M. Ammenwerth, H. Timme, F. Gyger, R. Tao, I. Bloch, and J. Zeiher, Realization of a fast triple-magic all-optical qutrit in strontium-88, Phys. Rev. Lett. **135**, 143401 (2025).

[18] T. Roy, T. Kim, A. Romanenko, and A. Grassellino, Qudit-based quantum computing with SRF cavities at Fermilab, PoS **LATTICE2023**, 127 (2024).

[19] D. Janković, J.-G. Hartmann, M. Ruben, and P.-A. Hervieux, Noisy qudit vs multiple qubits: Conditions on gate efficiency for enhancing fidelity, npj Quantum Inf. **10**, 59 (2024).

[20] A. S. Nikolaeva, E. O. Kiktenko, and A. K. Fedorov, Efficient realization of quantum algorithms with qudits, EPJ Quantum Technol. **11**, 43 (2024).

[21] M. B. Mansky, S. L. n. Castillo, V. R. Puigvert, and C. Linnhoff-Popien, Near-optimal quantum circuit construction via Cartan decomposition, Phys. Rev. A **108**, 052607 (2023).

[22] E. M. Murairi, M. Sohaib Alam, H. Lamm, S. Hadfield, and E. Gustafson, Highly-efficient quantum fourier transformations for some non-Abelian groups, Phys. Rev. D **110**, 074501 (2024).

[23] Y. Wang, Z. Hu, B. C. Sanders, and S. Kais, Qudits and high-dimensional quantum computing, Front. Phys. **8**, 589504 (2020).

[24] M. Iqbal *et al.*, Qutrit toric code and parafermions in trapped ions, Nat. Commun. **16**, 6301 (2025).

[25] R. Majumdar, A. Saha, A. Chakrabarti, and S. Sur-Kolay, Intermediate qutrit-assisted Toffoli gate decomposition with quantum error correction, Quantum Inf. Process. **23**, 42 (2024).

[26] A. S. Nikolaeva, E. O. Kiktenko, and A. K. Fedorov, Generalized Toffoli gate decomposition using ququints: Towards realizing Grover's algorithm with qudits, Entropy **25**, 387 (2023).

[27] A. Saha and O. Khanna, Intermediate-qudit assisted improved quantum algorithm for string matching with an advanced decomposition of Fredkin gate, J. Appl. Log. - IfCoLog J. Log. Appl. **12**, 63 (2025).

[28] E. Champion, Z. Wang, R. W. Parker, and M. S. Blok, Efficient control of a transmon qudit using effective spin-7/2 rotations, Phys. Rev. X **15**, 021096 (2025).

[29] E. O. Kiktenko, A. S. Nikolaeva, P. Xu, G. V. Shlyapnikov, and A. K. Fedorov, Scalable quantum computing with qudits on a graph, Phys. Rev. A **101**, 022304 (2020).

[30] T. Roy, Z. Li, E. Kapit, and D. Schuster, Two-qutrit quantum algorithms on a programmable superconducting processor, Phys. Rev. Appl. **19**, 064024 (2023).

[31] C. T. Hann, G. Lee, S. Girvin, and L. Jiang, Resilience of quantum random access memory to generic noise, PRX Quantum **2**, 020311 (2021).

[32] S. Zhu, A. Sundaram, and G. H. Low, Unified architecture for a quantum lookup tables, Phys. Rev. Res. **7**, 043230 (2025).

[33] S. Malpathak, S. D. Kallullathil, and A. F. Izmaylov, Simulating vibrational dynamics on bosonic quantum devices, J. Phys. Chem. Lett. **16**, 1855 (2025).

[34] E. Kaxiras and J. D. Joannopoulos, *Quantum Theory of Materials* (Cambridge University Press, 2019).

[35] L. Lin and J. Lu, *A Mathematical Introduction to Electronic Structure Theory* (SIAM, 2019).

[36] R. Babbush, D. W. Berry, R. Kothari, R. D. Somma, and N. Wiebe, Exponential quantum speedup in simulating coupled classical oscillators, Phys. Rev. X **13**, 041041 (2023).

[37] S. Chicco, G. Allodi, A. Chiesa, E. Garlatti, C. D. Buch, P. Santini, R. De Renzi, S. Piligkos, and S. Carretta, Proof-of-concept quantum simulator based on molecular spin qudits, J. Am. Chem. Soc. **146**, 1053 (2024).

[38] D. Tancara and F. Albarrán-Arriagada, High-dimensional counterdiabatic quantum computing, npj Quantum Inf. **11**, 116 (2025).

[39] G. Bottrill, M. Pandey, and O. Di Matteo, Exploring the potential of qutrits for quantum optimization of graph coloring, in *2023 International Conference on Quantum Computing and Engineering* (IEEE, Bellevue, WA, USA, 2023).

[40] S. Bravyi, A. Kliesch, R. Koenig, and E. Tang, Hybrid quantum-classical algorithms for approximate graph coloring, Quantum **6**, 678 (2022).

[41] A. Saha, T. Chatterjee, A. Chattopadhyay, and A. Chakrabarti, Intermediate qutrit-based improved quantum arithmetic operations with application on financial derivative pricing, arXiv:2205.15822.

[42] M. Chizzini, F. Tacchino, A. Chiesa, I. Tavernelli, S. Carretta, and P. Santini, Qudit-based quantum simulation of fermionic systems, Phys. Rev. A **110**, 062602 (2024).

[43] O. Ogunkoya, J. Kim, B. Peng, A. B. Özgüler, and Y. Alexeev, Qutrit circuits and algebraic relations: A pathway to efficient spin-1 Hamiltonian simulation, Phys. Rev. A **109**, 012426 (2024).

[44] S. Choi, N. Y. Yao, and M. D. Lukin, Dynamical engineering of interactions in qudit ensembles, Phys. Rev. Lett. **119**, 183603 (2017).

[45] L. Bassman Oftelie, K. Klymko, D. Liu, N. M. Tubman, and W. A. de Jong, Computing free energies with fluctuation relations on quantum computers, Phys. Rev. Lett. **129**, 130603 (2022).

[46] A. Young, Quantum spin systems, arXiv:2308.07848.

[47] E. Gustafson *et al.*, Large scale multi-node simulations of $\mathbb{Z}_2$ gauge theory quantum circuits using Google Cloud Platform, in 2021 IEEE/ACM Second International Workshop on Quantum Computing Software (QCS) (IEEE, St. Louis, MO, USA, 2021).

[48] E. Gustafson, Prospects for simulating a qudit based model of (1 + 1)D scalar QED, Phys. Rev. D **103**, 114505 (2021).

[49] D. González-Cuadra, T. V. Zache, J. Carrasco, B. Kraus, and P. Zoller, Hardware efficient quantum simulation of non-Abelian gauge theories with qudits on Rydberg platforms, Phys. Rev. Lett. **129**, 160501 (2022).

[50] P. P. Popov, M. Meth, M. Lewenstein, P. Hauke, M. Ringbauer, E. Zohar, and V. Kasper, Variational quantum simulation of U(1) lattice gauge theories with qudit systems, Phys. Rev. Res. **6**, 013202 (2024).

[51] H. C. Nguyen, B. G. Bach, T. D. Nguyen, D. M. Tran, D. V. Nguyen, and H. Q. Nguyen, Simulating neutrino oscillations on a superconducting qutrit, Phys. Rev. D **108**, 023013 (2023).

[52] G. Calajò, G. Magnifico, C. Edmunds, M. Ringbauer, S. Montangero, and P. Silvi, Digital quantum simulation of a (1+1)D SU(2) lattice gauge theory with ion qudits, PRX Quantum **5**, 040309 (2024).

[53] M. Illa, C. E. P. Robin, and M. J. Savage, Qu8its for quantum simulations of lattice quantum chromodynamics, Phys. Rev. D **110**, 014507 (2024).

[54] T. V. Zache, D. González-Cuadra, and P. Zoller, Fermion-qudit quantum processors for simulating lattice gauge theories with matter, Quantum **7**, 1140 (2023).

[55] E. J. Gustafson, Y. Ji, H. Lamm, E. M. Murairi, S. O. Perez, and S. Zhu, Primitive quantum gates for an SU(3) discrete subgroup: $\Sigma(36 \times 3)$, Phys. Rev. D **110**, 034515 (2024).

[56] L. Spagnoli *et al.*, Collective neutrino oscillations in three flavors on qubit and qutrit processors, Phys. Rev. D **111**, 103054 (2025).

[57] B. Eastin and E. Knill, Restrictions on transversal encoded quantum gate sets, Phys. Rev. Lett. **102**, 110502 (2009).

[58] M. A. Nielsen and I. L. Chuang, *Quantum Computation and Quantum Information: 10th Anniversary Edition* (Cambridge University Press, 2010).

[59] C. Gidney, N. Shutty, and C. Jones, Magic state cultivation: Growing T states as cheap as CNOT gates, arXiv:2409.17595.

[60] A. Wills, M.-H. Hsieh, and H. Yamasaki, Constant-overhead magic state distillation, Nat. Phys. **21**, 1842 (2025).

[61] T. J. Yoder, Universal fault-tolerant quantum computation with Bacon-Shor codes, arXiv:1705.01686.

[62] G. Zhu, S. Sikander, E. Portnoy, A. W. Cross, and B. J. Brown, Non-Clifford and parallelizable fault-tolerant logical gates on constant and almost-constant rate homological quantum LDPC codes via higher symmetries, arXiv:2310.16982.

[63] N. Rengaswamy, R. Calderbank, M. Newman, and H. D. Pfister, On optimality of CSS codes for transversal T, IEEE J. Sel. Areas Inf. Theory **1**, 499 (2020).

[64] O. Parzanchevski and P. Sarnak, Super-golden-gates for PU(2), Adv. Math. **327**, 869 (2018).

[65] T. R. Blackman and Z. Stier, Fast navigation with icosahedral golden gates, arXiv:2205.03007.

[66] E. Kubischta and I. Teixeira, A family of quantum codes with exotic transversal gates, Phys. Rev. Lett. **131**, 240601 (2023).

[67] A. Bocharov, Y. Gurevich, and K. M. Svore, Efficient decomposition of single-qubit gates into V basis circuits, Phys. Rev. A **88**, 012313 (2013).

[68] G. H. Low, V. Kliuchnikov, and L. Schaeffer, Trading T gates for dirty qubits in state preparation and unitary synthesis, Quantum **8**, 1375 (2024).

[69] S. Evra and O. Parzanchevski, Ramanujan complexes and golden gates in PU(3), Geom. Funct. Anal. **32**, 193 (2022).

[70] E. Kubischta and I. Teixeira, Quantum codes from twisted unitary t-groups, Phys. Rev. Lett. **133**, 030602 (2024).

[71] M. Howard and J. Vala, Qudit versions of the qubit $\pi/8$ gate, Phys. Rev. A **86**, 022316 (2012).

[72] E. T. Campbell, H. Anwar, and D. E. Browne, Magic-state distillation in all prime dimensions using quantum Reed-Muller codes, Phys. Rev. X **2**, 041021 (2012).

[73] S. Prakash, A. Jain, B. Kapur, and S. Seth, Normal form for single-qutrit Clifford+T operators and synthesis of single-qutrit gates, Phys. Rev. A **98**, 032304 (2018).

[74] S. Prakash, A. R. Kalra, and A. Jain, A normal form for single-qudit Clifford+T operators, Quantum Inf. Process. **20**, 341 (2021).

[75] D. Amaro-Alcalá, B. C. Sanders, and H. de Guise, Randomised benchmarking for universal qudit gates, New J. Phys. **26**, 073052 (2024).

[76] A. R. Kalra, M. Mosca, and D. Valluri, Synthesis and arithmetic of single qutrit circuits, Quantum **9**, 1647 (2025).

[77] A. N. Glaudell, N. J. Ross, J. van de Wetering, and L. Yeh, Exact synthesis of multiqutrit Clifford-cyclotomic circuits, Electron. Proc. Theor. Comput. Sci. **406**, 44 (2024).

[78] S. Evra and O. Parzanchevski, Arithmeticity, thinness and efficiency of qutrit Clifford+T gates, arXiv:2401.16120.

[79] A. Bocharov, A note on optimality of quantum circuits over metaplectic basis, Quant. Inf. Comput. **18**, 0001 (2018).

[80] A. N. Glaudell, N. J. Ross, J. van de Wetering, and L. Yeh, Qutrit metaplectic gates are a subset of Clifford+T, Leibniz Int. Proc. Inf. **232**, 12:1 (2022).

[81] C. M. Dawson and M. A. Nielsen, The Solovay-Kitaev algorithm, Quant. Inf. Comput. **6**, 081 (2006).

[82] G. Kuperberg, Breaking the cubic barrier in the Solovay-Kitaev algorithm, arXiv:2306.13158.

[83] A. W. Harrow, B. Recht, and I. L. Chuang, Efficient discrete approximations of quantum gates, J. Math. Phys. **43**, 4445 (2002).

[84] J. Bourgain and A. Gamburd, A spectral gap theorem in SU(d), J. Eur. Math. Soc. **14**, 1455 (2012).

[85] A. N. Glaudell, N. J. Ross, and J. M. Taylor, Canonical forms for single-qutrit Clifford+T operators, Ann. Phys. (NY) **406**, 54 (2019).

[86] V. Kliuchnikov, D. Maslov, and M. Mosca, Fast and efficient exact synthesis of single-qubit unitaries generated by Clifford and T gates, Quantum Info. Comput. **13**, 607 (2013).

[87] K. L. Manders and L. Adleman, NP-complete decision problems for binary quadratics, J. Comput. Syst. Sci. **16**, 168 (1978).

[88] N. J. Ross and P. Selinger, Optimal ancilla-free Clifford+T approximation of Z-rotations, Quant. Inf. Comput. **16**, 0901 (2016).

[89] A. Bocharov, M. Roetteler, and K. M. Svore, Efficient synthesis of universal repeat-until-success quantum circuits, Phys. Rev. Lett. **114**, 080502 (2015).

[90] A. Bocharov, X. Cui, V. Kliuchnikov, and Z. Wang, Efficient topological compilation for a weakly integral anyonic model, Phys. Rev. A **93**, 012313 (2016).

[91] A. Horn, Doubly stochastic matrices and the diagonal of a rotation matrix, Am. J. Math. **76**, 620 (1954).

[92] J. d. A. Bezerra, A note on completion to the unitary matrices, Linear Multilinear Algebra **69**, 1825 (2021).

[93] J. W. S. Cassels, *An Introduction to the Geometry of Numbers* (Springer Berlin, Heidelberg, 1959).

[94] B. Cha and D. H. Kim, Intrinsic diophantine approximation on circles and spheres, Mathematika **70**, e12228 (2024).

[95] V. Kliuchnikov, Synthesis of unitaries with Clifford+T circuits, arXiv:1306.3200.

[96] S. Li, Concise formulas for the area and volume of a hyperspherical cap, Asian J. Math. Stat. **4**, 66 (2010).

[97] K. Matsumoto and K. Amano, Representation of quantum circuits with Clifford and $\pi/8$ gates, arXiv:0806.3834.

[98] V. V. Shende, I. L. Markov, and S. S. Bullock, Minimal universal two-qubit controlled-not-based circuits, Phys. Rev. A **69**, 062321 (2004).

[99] J. Unmuth-Yockey, J. Zhang, A. Bazavov, Y. Meurice, and S.-W. Tsai, Universal features of the Abelian Polyakov loop in $1+1$ dimensions, Phys. Rev. D **98**, 094511 (2018).

[100] J. F. Unmuth-Yockey, Gauge-invariant rotor Hamiltonian from dual variables of 3D U(1) gauge theory, Phys. Rev. D **99**, 074502 (2019).

[101] E. Gustafson, Noise improvements in quantum simulations of sQED using qutrits, arXiv:2201.04546.

[102] D. M. Kürkçüoglu, H. Lamm, and A. Maestri, Qudit gate decomposition dependence for lattice gauge theories, arXiv:2410.16414.

[103] N. E. Tunali, K. R. Narayanan, J. J. Boutros, and Y.-C. Huang, Lattices over Eisenstein integers for compute-and-forward, IEEE Trans. Inf. Theory **61**, 5306 (2015).

[104] J. P. Buhler, H. W. Lenstra, and C. Pomerance, Factoring integers with the number field sieve, in *The Development of the Number Field Sieve* (Springer Berlin, Heidelberg, 1993), pp. 50–94.